Child Palm-ID: Contactless Palmprint Recognition for Children

Akash Godbole[1], Steven A. Grosz[2] and Anil K. Jain[3], *Life Fellow, IEEE*

Michigan State University

{[1]godbole1, [2]groszste, [3]jain}@cse.msu.edu

May 10, 2023

Abstract

Effective distribution of nutritional and healthcare aid for children, particularly infants and toddlers, in some of the least developed and most impoverished countries of the world, is a major problem due to the lack of reliable identification documents. Biometric authentication technology has been investigated to address child recognition in the absence of reliable ID documents. We present a mobile-based contactless palmprint recognition system, called Child Palm-ID, which meets the requirements of usability, hygiene, cost, and accuracy for child recognition. Using a contactless child palmprint database, Child-PalmDB1, consisting of 19,158 images from 1,020 unique palms (in the age range of 6 mos. to 48 mos.), we report a TAR=94.11% @ FAR=0.1%. The proposed Child Palm-ID system is also able to recognize adults, achieving a TAR=99.4% on the CASIA contactless palmprint database and a TAR=100% on the COEP contactless adult palmprint database, both @ FAR=0.1%. These accuracies are competitive with the SOTA provided by COTS systems. Despite these high accuracies, we show that the TAR for time-separated child-palmprints is only 78.1% @ FAR=0.1%.

1 Introduction

In 2020, 22% of the world's 680 million children [1], under the age of 5 years, were physically stunted due to malnourishment and lack of adequate medication[1]. A majority of these children live in developing or least developed countries where healthcare facilities and other resources are scarce. To address this problem, many in-

a) Child face images from Child-PalmDB2

b) Contactless child palmprints from Child-PalmDB2

Figure 1: Example face (a) and corresponding contactless palmprint images (b) in Child-PalmDB2 contactless palmprint database.

ternational organizations such as the World Health Organization (WHO)[2], Bill and Melinda Gates Foundation (BMGF)[3] and the World Food Programme (WFP)[4] have made substantial efforts to reduce the rate of malnourishment as well as improve vaccination coverage among this vulnerable population. However, the lack secure government-issued identification makes it difficult to authenticate the recipient of the services and curtail the occurence of fraud.

Biometrics has received significant attention for the identification of children. However, biometrics-based

---

[1]https://www.who.int/data/gho/data/themes/topics/joint-child-malnutrition-estimates-unicef-who-wb

[2]https://www.afro.who.int/news/strategic-plan-reduce-malnutrition-africa-adopted-who-member-states

[3]https://www.gatesfoundation.org/our-work/programs/global-growth-and-opportunity/nutrition

[4]https://www.wfp.org/nutrition

Table 1: Summary of literature on biometric recognition of children

Authors	Modality	Age Group (# Subjects)	Sensor	Accuracy[*]	Limitations
Jain et al. [2]	Fingerprint	0-5 yrs (309)	Contact-based commercial and custom sensors	TAR=95% @ FAR=0.1% using undisclosed matcher	Recognition algorithm unknown
Saggese et al. [3]	Fingerprint	0-18 mos. (504)	Custom contactless sensor	TAR=96.2% @ FAR=0.1% using Verifinger[**]	Complex fingerprint reader design
Engelsma et al. [4]	Fingerprint	8-16 weeks (315)	Custom contactless sensor	TAR=92.8% @ FAR=0.1% using in-house matcher	Slow data acquisition
Kalisky et al. [5]	Fingerprint	0-329 days (494)	Custom contactless sensor	TAR=77.0% @ FAR=0.1% using Verifinger[**]	Low time-separated accuracy
Liu [6]	Footprint	1-9 mos. (60)	Contact-based commercial sensor	TAR=60% @ FAR=0.01% using in-house matcher	Train and test set from same acquisition
Kotzerke et al. [7]	Footprint	2 days-6 mos. (60)	DSLR Camera	EER=22.22% using in-house matcher	Lack of high quality data
Yambay et al. [8]	Toe print	4-13 years (177)	Commercial contact-based sensor	EER=2.5% using Verifinger[**]	Larger age group
Uhl and Wild [9]	Palmprint	3 yrs-18 yrs (301)	Flatbed scanner[1]	EER=4.63% using in-house matcher	Larger age group
Ramacha-ndra et al. [10]	Contactless Palmprint	6-36 hours (50)	Smartphone camera	EER=0.31% using pre-trained AlexNet	Insufficient data for training and testing
Rajaram et al. [11]	Contactless Palmprint	3 mos-8 yrs (100)	Smartphone camera	EER=0.02% using in-house matcher	Train and test set from same acquisition
This paper	Contactless Palmprint	6 mos. - 4 yrs (515)	Smartphone camera	TAR=94.11% @ FAR=0.1%	Low time-separated accuracy

[*] *The studies listed above have used different evaluation metrics. Specifically, child fingerprint recognition and footprint recognition studies report TAR(%) at FAR = 0.1% (0.01%) and the studies on toe prints and contactless palmprints report EER.*
[**] *Version number unknown.*
[1] *The hand was placed at a stand-off above the flat-bed.*

identification solutions for children have yet to meet the requirements for field deployment, namely i) low-cost acquisition, ii) high accuracy, iii) robustness to capture environment (e.g. dust, humidity, and temperature), and iv) large throughput. Indeed, large-scale biometric identification systems in use today were not designed for use by very young children (infants and toddlers)[5]. The largest civil biometric system in the world, Aadhaar, only enrolls Indian residents over the age of 5 [12]. This leaves a population of almost 118 million young children unaccounted for in India alone.

In addition to the above requirements for child biometric recognition, it is important to note that a biometric trait must meet the *persistence* and *individuality* requirements for the population under consideration [13]. These requirements make it difficult to justify using face biometric since a child's face (both appearance and shape) changes significantly during the first few years after birth. A few studies have suggested using footprints and toe prints, but they neither satisfy the real-time acquisition requirement nor the ergonomics. Iris images are difficult to capture if the child is sleeping or crying. Further, capturing iris may require the operator to forcibly open the child's eye which may make the parents uncomfortable. These limitations, paired with the rise of global virus outbreaks and concerns about hygiene, has motivated a push to develop biomteric systems that do not require physical contact with any capture surface [14, 15, 16]. To satisfy all these requirements, we propose contactless palmprints as a cost-effective and robust solution for child identification. The proposed Child Palm-ID does not even require custom sensors, as in the case of fingerprint, footprint and iris since smartphone cameras have sufficient resolution to capture contactless palmprint images of children.

Table 1 shows some of the more prominent studies on biometric recognition for children. The fingerprint modality has been the popular choice thus far but recent studies have shown a trend towards contactless palmprints. The primary obstacle in contactless palmprint recognition for children is lack of training and evaluation data, both in terms of number of unique identities and longitudinal (time-separated) collections. Therefore, as part of this study, we collect three new datasets containing

over 60,000 images from 1,824 unique child palms and 1,227 unique adult palms, called Child-PalmDB1 (August 2022), Child-PalmDB2 (January 2023) and Adult-PalmDB2 (January 2023), respectively (Fig. 4). Child-PalmDB1 and Child-PalmDB2 contain 159 common subjects (318 palms) for time-separated verification that we refer to as Child CrossDB.

Prior attempts at palmprint-based recognition for children focused on newborns and infants (less than 12 mos. old). These studies faced a number of challenges in palmprint capture of "uncooperative" subjects [18]. To keep the child recognition problem tractable, we focus on children between 6 mos. to 48 mos. old. Child development studies [19] report that starting at the age of 12 mos., a child can follow instructions such as opening the fist and holding the palm in front of a mobile phone camera. This age group is also of interest to Aadhaar 2.0 [20], where one of the objectives is to lower the enrolment age which has been set at 5 yrs. since the inception of the program in 2009.

A contactless palmprint recognition system demands robustness to intra-class variability due to pose variations in palmprint images. The proposed Child Palm-ID addresses this problem by predicting landmarks on palm images coupled with a re-alignment of Regions of Interest (ROI) via a Thin Plate Spline (TPS) re-alignment module. Concretely, the contributions of this study are as follows:

- A mobile-based contactless palmprint recognition system, Child Palm-ID, designed and prototyped for infants and toddlers.
- Keypoint detection and TPS re-alignment modules to handle large non-linear distortion and pose variations.
- Collection of Child-PalmDB1 and Child-PalmDB2 containing 1,824 unique child palms, and Adult-PalmDB2 containing 1,227 unique adult palms. These databases will be released once this paper is accepted for publication.
- Longitudinal contactless palmprint verification on Child CrossDB, a time-separated (∼5 mos.) contactless child palmprint database containing 12,720 images from 318 unique palms.
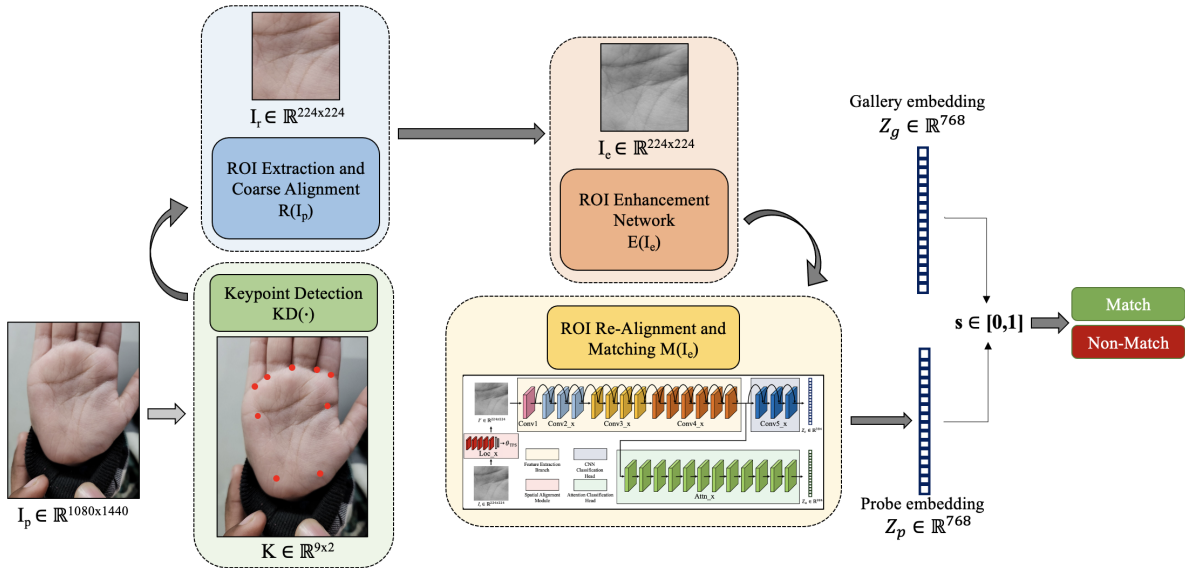
---

[5]According to the Center for Disease Control (CDC), infants are between the ages of 0-1 yrs. and toddlers are between 2-3 yrs. https://www.cdc.gov/ncbddd/childdevelopment/positiveparenting/index.html

Figure 2: A schematic diagram of the operational pipeline of Child Palm-ID. The input image I_p is passed to the keypoint detection network $KD(\cdot)$. The coarse alignment between the probe and gallery images is based on a homographic transformation, followed by the AFR-Net architecture with a TPS unwarping module. The AFR-Net architecture diagram is adapted from [17].

2 Related Work

Contactless palmprint recognition consists of the following stages: i) Region of Interest (ROI) extraction, ii) ROI alignment and enhancement and iii) ROI comparison. See Fig. 2. The predominant effort in the literature has been in building palmprint recognition systems for adults [23, 24, 25, 26, 27, 28, 29, 30, 31] while the focus on children has been limited [11, 10].

2.1 ROI Extraction

Due to the potential of large pose variation in contactless palmprint image acquisition, it is important to obtain a consistent region of interest (ROI) across all the captured images.

Depending on the nature of palmprint image acquisition, the ROI extraction method may vary. Handcrafted methods include binarizing the image to detect the finger valleys and using them to locate a square region on the palmar surface [24]. This method may fail, for instance, if the fingers of the hand are not fully extended and separated from each other.

The acquisition of child palmprints may not always adhere to the above pose constraint requirement due to the continual development of fine motor control children have on their hands and fingers. Therefore, the proposed Child Palm-ID uses a deep-learning approach to predict a set of *landmarks* to localize the ROI via a homographic transformation, an approach commonly used in face recognition [32, 33] with larger pose variations.

We consider this landmark-based ROI to be *coarsely aligned*, meaning it may require re-alignment for an accurate comparison with ROIs extracted from other palms. This will be further elaborated in sections 4.1 and 4.2.

2.2 ROI Alignment

Adult palmprint recognition systems have utilized the principal lines, also referred to as palmar creases [34, 35], for the re-alignment of ROIs [36, 37]. This method is effective provided that the palm capture adheres to pose constraints mentioned earlier.

Recent advances in fingerprint and face recognition have turned to the use of Spatial Transformer Networks (STN), to predict alignment parameters that maximize
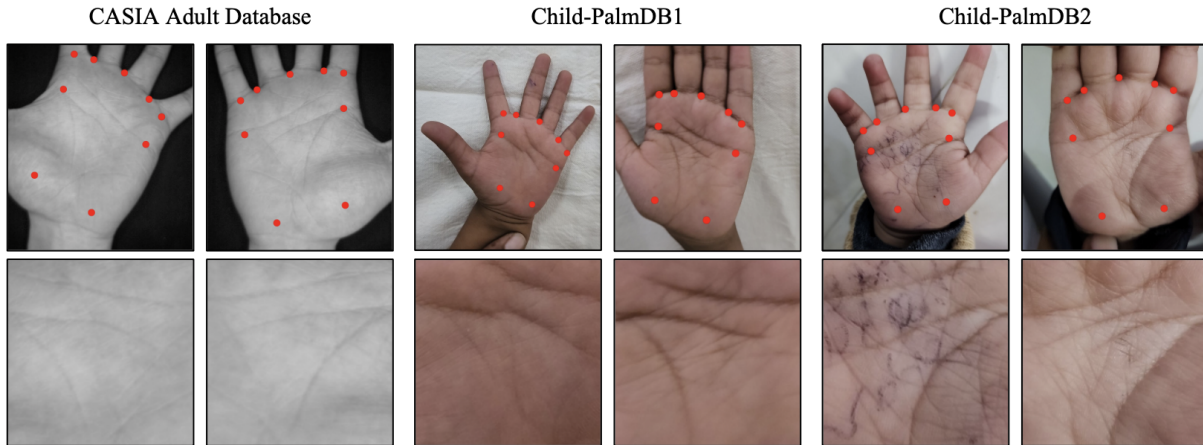
Figure 3: Nine predicted keypoints overlaid (shown in red, top row) on the palmprint images from the CASIA Palmprint Image Database [21], Child-PalmDB1 and Child-PalmDB2. The bottom row shows the ROIs extracted via homographic transformation.
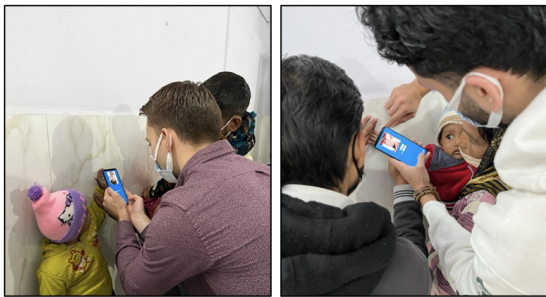

Figure 4: Data collection camp in Dayalbagh, India, January 2023. The authors are collecting palmprint images using the PalmMobile SDK [22].

the recognition accuracy [38, 39, 17]. Additionally, fine-tuned, non-linear alignment using a Thin Plate Spline (TPS) STN has shown even higher recognition performance in more unconstrained scenarios such as 3D facial recognition and contact-to-contactless fingerprint matching [40, 41].

In this paper, we implement a semi-supervised TPS STN module that learns a non-linear distortion field for a coarsely aligned ROI for improved accuracy of Child Palm-ID.

2.3 ROI Matching

Methods of comparing two palmprint images range from mathematical operations such as Fourier Transforms [42] to learned embeddings from deep networks. A large proportion of recent studies have utilized deep networks to achieve compact embeddings (template) for high throughput, high accuracy and robustness compared to many handcrafted features [23, 43, 44, 45].

3 Databases

We use a number of adult contactless palmprint databases available in the public domain, namely Tongji Adult Palmprint Database [24], CASIA Adult Palmprint Database [21] , CASIA Multispectral Database [46] , COEP Adult Palmprint database [47][6] and the Sapienza University Mobile Palmprint Datbase (SMPD) [48]. We also utilize a private contactless palmprint video database containing 25-second video clips of 1,016 unique palms[7]. These databases were collected using different capture devices and different image resolutions (from 600x800 px. to 3264x2448 px.).

The ages of the children in Child-PalmDB1 and Child-PalmDB2 range from a minimum of 6 mos. to a maximum of 48 mos. Child-PalmDB1 was collected in August 2022 whereas Child-PalmDB2 and Adult-PalmDB2 were collected in January 2023[8]. There are 159 overlapping subjects (excluded from the training set) in Child-PalmDB1 and Child-PalmDB2, called Child CrossDB,

---

[6]The COEP database contains 17 identities (136 images) that are mislabelled, which were excluded from the evaluation results.

[7]We are unable to disclose details of this database due to NDA.

[8]Child-PalmDB1, Child-PalmDB2 and Adult-PalmDB2 were collected at Saran Ashram Hospital in Dayalbagh, India under approved IRB from both the hospital and the authors' institution.

a) Contactless palmprint images of children from Child-PalmDB2

b) Contactless palmprint images of adults from Adult-PalmDB2

Figure 5: Sample contactless palmprint images from (a) Child-PalmDB2 and (b) Adult-PalmDB2. For the child palmprint images, the age of the child is also included.

Table 2: Details of databases used in this study

Training Database[*]	# Unique Palms	Total # images
Tongji Adult [24]	600	12,000
CASIA Multispectral [46]	200	7,200
Child-PalmDB2[1]	1,122	18,277
Adult-PalmDB2[1]	1,227	22,548
SMPD [48] [†]	92	3,677
Private Database [3]	1,016	28,748
Testing Database	**# Unique Palms**	**Total # images**
CASIA Adult [21]	614	5,502
COEP Adult [47]	168	1,344
Child-PalmDB1[2]	1,020	19,158
Child CrossDB	318	12,720

[1] *Collected by authors. Will be released once the paper is accepted for publication.*
[2] *Collected by authors. Already in the public domain but anonymized for blind review.*
[3] *We extract individual frames from the video clip of each unique palm.*
[*] *Training and testing databases are disjoint.*
[†] *https://www.kaggle.com/datasets/mahdieizadpanah/sapienza-university-mobile-palmprint-databasesmpd*

4 Child Palm-ID Framework

The operational pipeline of Child Palm-ID can be divided into four major components: i) Keypoint detection, ii) ROI extraction, iii) ROI enhancement, and iv) ROI re-alignment and matching. Fig. 2 shows a high-level schematic of Child Palm-ID.

4.1 Keypoint Detection

The keypoint detection module $KD(\cdot)$ uses a ResNet-18 (see Table 2 for training set) architecture with two fully connected layers inserted at the end to predict 9 keypoints $K \in \mathbb{R}^{9x2}$ in the input image (I_p); these keypoints are used to extract the coarsely aligned ROI. These 9 keypoints (fig 6) provide a degree of symmetry between the right and left hand while encompassing the the palm boundary containing salient information for a robust ROI. As groundtruth for training $KD(\cdot)$, we use the keypoints generated by the COTS system. An MSE objective function is minimized to predict the keypoints. Fig. 3 shows the predicted keypoints from $KD(\cdot)$ overlaid on the palmprint images on three databases. The predicted keypoints along with the

providing an avenue to explore time-separated contactless palmprint recognition performance for children. The palmprint images were collected using the Armatura PalmMobile SDK android application installed on a Samsung Galaxy S22 [22]. The palm images for each child were collected with variations in roll, pitch, and yaw to best simulate a real world collection scenario.

Table 2 shows the number of subjects and number of images in each of the databases[9] used in this study as well as training and evaluation datasets. For the age groups of 6-12 mos., 12-24 mos. and 24-48 mos., Child-PalmDB1 contains 73, 161 and 230 subjects[10], respectively and Child-PalmDB2 contains 105, 202 and 375 subjects, respectively. For each subject, we collect images from both palms. So, the total number of unique palms is 2,142, including the 318 common palms between the two databases.

---

[9]The authors are aware of PolyU-IITD and IITD Touchless Palmprint Database but despite our repeated requests, we were unable to obtain access to them.

[10]Age information in Child-PalmDB1 is available for 444 subjects out of 515 subjects.

a) Input image with predicted keypoints (red) and ROI (white)

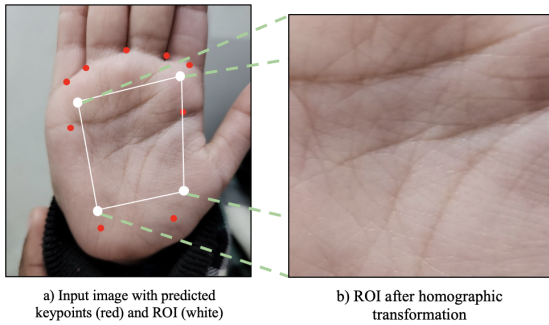b) ROI after homographic transformation

Figure 6: Extracted keypoints (a) along with the ROI (b) after the coarse alignment. The polygon in (a) is an inverse homographic transformation of the four image vertices of (b) on (a) and represents the palmar region captured in the ROI.
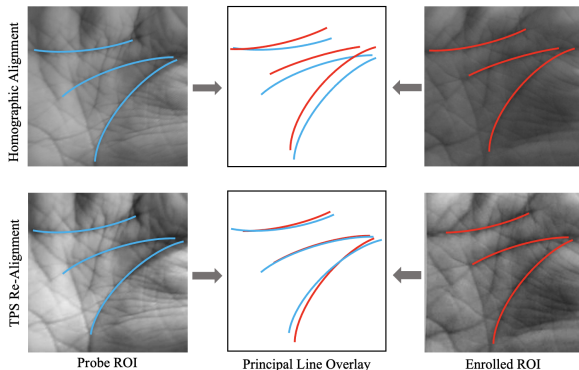

Figure 7: Benefit of the TPS re-alignment. The ROIs in the bottom row are the re-aligned counterparts of the coarsely aligned ROIs in the top row.

input image serve as input to the ROI extraction module.

4.2   ROI extraction

Accurate alignment of palmprint images to a consistent coordinate system is essential to extract a robust, albeit coarsely aligned, ROI. To homogenize the coordinate system, a set of 9 destination points D are selected to perform a 9-point homographic transformation $H(\cdot)$ between K and D yielding a perspective transform matrix θ_h. The ROI module $R(\cdot)$ applies θ_h to I_p to get a warped image I_p^w; a 224 x 224 cropped image C is extracted yielding the coarsely aligned ROI, I_r (eqs. 1, 2, 3).

$$\theta_h = H(K, D) \qquad (1)$$

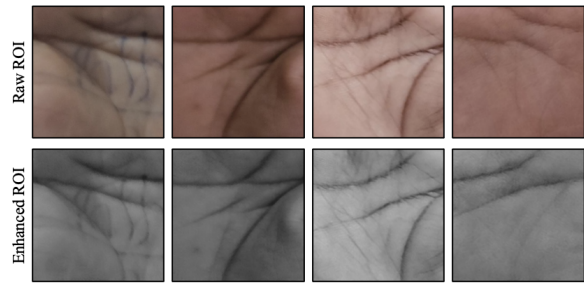$$I_p^w = R(I_p; \theta_h) \qquad (2)$$

Figure 8: Extracted ROIs (top row) and the corresponding enhanced ROIs (bottom row).

$$I_r = C(I_p^w, 224) \qquad (3)$$

4.3   ROI enhancement

We utilize the autoencoder network designed to enhance poor quality latent fingerprints in LFR-Net [49] and adapt it to enhance contactless palmprints. Due to the unconstrained nature of contactless palm capture, many of the captured images exhibit very poor ridge contrast, motion blur, and other degradations. To help mitigate these challenges, for training the autoencoder we simulated low quality palm images by, for example, blurring and downsampling as data augmentations. The autoencoder is trained via an MSE loss between the high quality palmprint inputs and the reconstructed outputs of the enhancement network. Example enhanced images are shown in Fig. 8 and the benefit of the enhancement network is shown quantitatively in the ablation study in section 5.2.

4.4   Re-Alignment and Matching

The feature extraction and matching architecture of Child Palm-ID is based on AFR-Net [17], a fingerprint recognition model based on ResNet50 [50] and Vision Transformers (ViT) [51]. AFR-Net uses an STN to predict an affine alignment of the input images. We modify the STN to predict a TPS alignment that applies a non-linear, learned, distortion field θ_{TPS} to the coarsely aligned palmprint ROIs (I_r) producing an aligned ROI, I' (eq. 4).

$$I' = T(I_r; \theta_{TPS}) \qquad (4)$$

A learned TPS network has been shown to boost performance in fingerprint and face matching [41, 40]. Fig. 7 shows the improved alignment between two ROIs after applying $T(I_r)$. Affirming the intuition behind the use of

7

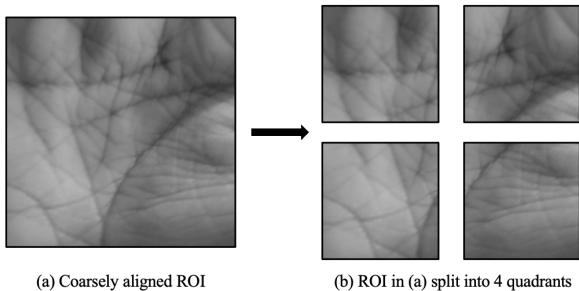(a) Coarsely aligned ROI   (b) ROI in (a) split into 4 quadrants

Figure 9: The coarsely aligned and enhanced ROI (a) and its 4 quadrants (b). A model is trained for each quadrant and the whole ROI. Final similarity score is a fusion of the 5 model scores.

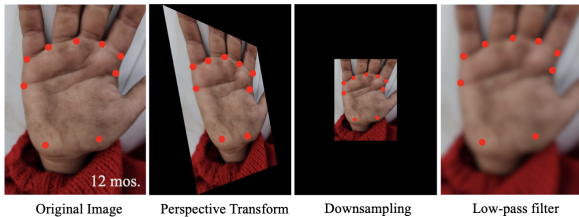Original Image   Perspective Transform   Downsampling   Low-pass filter

Figure 10: Examples of data augmentations for Child Palm-ID training. Rotation and translation augmentations are not shown.

$T(\cdot)$, a significant boost in recognition performance was observed compared to the use of the pre-existing STN in AFR-Net (from TAR = 73.8% to TAR = 88.3%, both at FAR = 0.1%. See Table 4.).

The probe and gallery embeddings Z_p and Z_g, respectively, are compared to obtain a similarity score $s \in [0, 1]$ (eq. 5).

$$s = Z_p^T \cdot Z_g, \in [0, 1] \qquad (5)$$

4.4.1 Ensemble of multi-patch embeddings

The crux of ensemble learning is utilizing multiple complimentary models that improve the overall performance of the system via different fusion techniques [52, 53]. We divide the 224x224 coarsely aligned, enhanced, ROIs into 4 quadrants (Fig. 9) and train an ensemble of models, one per quadrant to complement the model trained on the entire ROI. Using the ensemble of these five embeddings, we obtain a final similarity score based on mean score fusion. We show the quantitative benefit of the ensemble in the ablation study (Table 4).

4.5 Training Details

Child Palm-ID was trained using an ArcFace loss function with a margin of 1.5, learning rate of 1e-4, weight de-

cay of 2e-5, and polynomial learning rate decay function with a power of 3 and minimum learning rate of 1e-5. All models were trained with a batch size of 64 on a Nvidia GeForce RTX 2080Ti GPUs for 75 epochs. Furthermore, some key data augmentations (translation, rotation, scaling, blurring and perspective transforms) were randomly applied during the training process to improve the accuracy of the recognition system on images with large pose variations, commonly observed in child palmprint images. Fig. 10 shows examples of augmentations applied on a single palmprint image. Note that any number of these augmentations may be applied to a single image during training with a probability of $p = 0.5$.

5 Experimental Results

In this section we evaluate verification performance of Child Palm-ID and compare it to the baseline accuracy of the COTS system [22]. We report the accuracy on the entire Child CrossDB as well as the three age subgroups (6-12 mos., 12-24 mos. and 24-48 mos.) from Child-PalmDB1. Finally, we conduct an ablation study to examine the effects of re-alignment, learned enhancement, ensemble of embeddings and data augmentations on the performance of Child Palm-ID.

5.1 Verification Results

We report verification performance on four evaluation databases that were altogether kept separate from the training set (see Table 2). The recognition performance of the proposed Child Palm-ID is competitive with COTS[11]. We also report the longitudinal verification performance on the Child CrossDB containing the 159 subjects present in both Child-PalmDB1 and Child-PalmDB2 in Table 5. Images in Child CrossDB were not included in the training set.

It is instructive to notice the trend in performance of Child Palm-ID on different age groups. Intuitively, a recognition system would perform better on relatively older children since they are likely to be more cooperative during data acquisition. Child Palm-ID shows an accuracy of TAR=91.76% on children between the ages of 6 to 12 mos., TAR=95.74% on children between the ages of 12 to 24 mos. and TAR=98.86% on children in the age

---

[11]The architecture and training set for the COTS is not known to us and both the adult databases used for evaluation are in the public domain.

Table 3: TAR(%) @ FAR=0.1% of Child Palm-ID and COTS.

Database	Child Palm-ID	COTS [22]	Child Palm-ID + COTS
CPDB1[†] (all ages)	94.11	92.72	**94.46**
CPDB1[†] (6-12 mos.)	91.76	89.88	**92.48**
CPDB1[†] (12-24 mos.)	95.74	93.89	**96.12**
CPDB1[†] (24-48 mos.)	98.86	96.32	**98.97**
Child CrossDB [*]	78.1	78.22	**82.02**
CASIA Adult	99.4	100	100
COEP Adult[‡]	100	100	100

[†] *We abbreviate Child-PalmDB1 as CPDB1 in this table to save space.*
[‡] *17 mislabelled identities were removed.*
[*] *Child CrossDB was not included in the training set.*

group of 24-48 mos., all @ FAR=0.1%. Fig. 11 shows that Child Palm-ID outperforms the COTS system at FAR = 0.1% in each of the three evaluation age groups. We show an improvement by sum score fusion of Child Palm-ID and COTS, especially in the case of Child CrossDB at FAR=0.1% (see supplementary material for more details).

5.2 Ablation Study

In the ablation study, we examine the effects of the autoencoder enhancement module, TPS alignment module, multi-patch embeddings and data augmentations for training. The training datasets were fixed (Table 2) in these ablations. The results of the ablation study are shown in Table 4. The TPS re-alignment module in row 2 of Table 4, gives the biggest boost in accuracy on all the four evaluation databases. The image enhancement, ensemble of embeddings and data augmentations further boost the
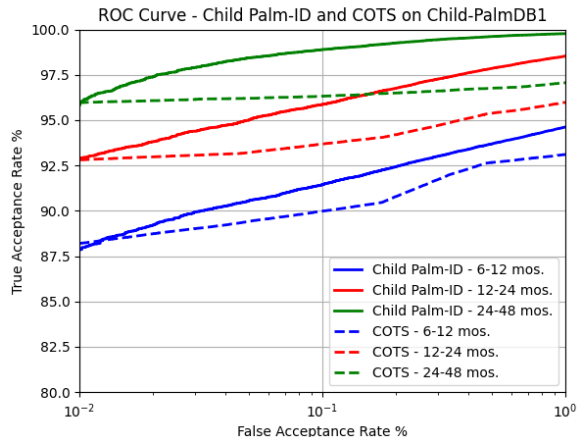

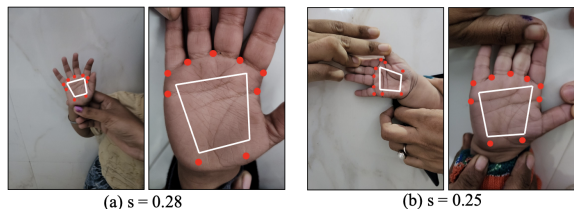Figure 11: ROC curves comparing the performance of Child Palm-ID against the COTS system [22] on Child-PalmDB1.

(a) s = 0.28   (b) s = 0.25

Figure 12: Failure cases of Child Palm-ID in Child CrossDB. For each genuine pair of images, the similarity score s is below the threshold of 0.46 at FAR = 0.1%. In both (a) and (b), the left image is from Child-PalmDB1 and the right image is from Child-PalmDB2.

accuracy.

5.3 Failure Cases

Fig. 14 shows the failure cases of Child Palm-ID when evaluated on Child-PalmDB1. The main reasons for failures are i) poor image quality and ii) severe variation in pose between two images.

Figs. 14(b) and 14(d) indicate the poor quality images that mainly arise due to the unexpected movement of the child's palm during the image acquisition process. The highlighted ROIs include partially closed fingers and incorrectly detected keypoints due to interference from the background. This can be mitigated by either implementing a palmprint quality metric to filter out such images or with adult supervision during palmprint acquisition. In Fig. 14(a), the subject's fist is partially closed and is partially occluded in Fig. 14(c). This leads to incorrect key-

Table 4: Ablation Study for Child Palm-ID. Results are reported as TAR (%) @ FAR = 0.1%

Modules Used					Evaluation Databases			
Coarse Alignment	Re-Alignment	Data Augmentation	Ensemble of Embeddings	Enhancement	Child-PalmDB1	CASIA Adult Database	COEP Adult Database	Child CrossDB
✓	✗	✗	✗	✗	73.8	92.4	91.6	66.56
✓	✓	✗	✗	✗	88.3	98.8	99.1	74.68
✓	✓	✓	✗	✗	92.43	99.1	100	76.67
✓	✓	✓	✓	✗	93.01	99.6	100	77.4
✓	✓	✓	✓	✓	94.11	99.4	100	78.1

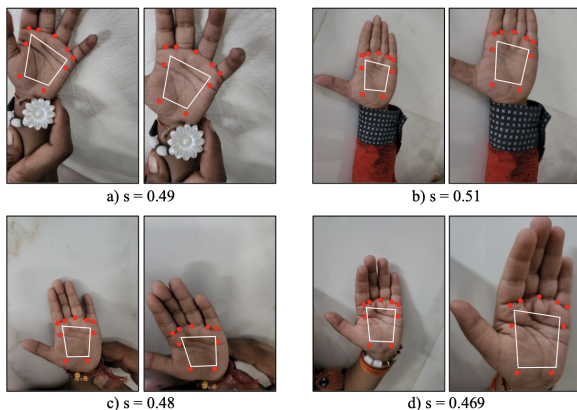a) s = 0.49   b) s = 0.51

c) s = 0.48   d) s = 0.469

Figure 13: Successful cases of Child Palm-ID in Child-PalmDB1. For each genuine pair of images, the similarity score s is above the threshold of 0.46 at FAR = 0.1%.

a) s = 0.31   b) s = 0.39

c) s = 0.16   d) s = 0.41

Figure 14: Failure cases of Child Palm-ID in Child-PalmDB1. For each genuine pair of images, the similarity score s is below the threshold of 0.46 at FAR = 0.1%.

point detection. However, Figs. 14(a) and 14(c) may also represent the genre of images that an untrained technician might acquire, thereby bearing some resemblance to an operational scenario.

Fig. 12 shows the failure cases of Child Palm-ID on Child CrossDB. This highlights the challenges in cross-dataset comparison where there are significant differences in standoff distance, lighting and rotation between two time-separated acquisitions.

5.4 Contactless child palmprint acquisition

As outlined previously, collecting palmprint images of a child is a challenging exercise that requires carefully designed protocols. From our experience, we recommend the following crucial guidelines for collection of high quality data:
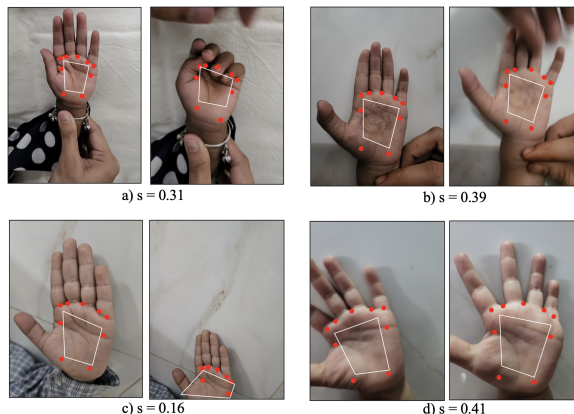
- Adult supervision to prevent unexpected movements of the child's palm.
- Fixed range of standoff distances and pose variations.
- Consistent and uniform lighting to reduce shadows and maintain high contrast in the images.

6   Conclusion and Future Work

Biometric recognition systems have made great strides over the past 20 years in terms of acquisition, accuracy, cost, and broad range of deployments ranging from mobile phone unlock to large-scale national ID. However, all these systems were designed to be used by adults. Yet there are numerous social good tasks ranging from eradicating vaccine preventable diseases to child malnutrition where biometric recognition can play a significant role to

prevent misery and loss of life.

We have designed and prototyped Child Palm-ID, a contactless mobile-based palmprint recognition system geared towards children. We have evaluated verification performance of Child Palm-ID on both child as well as adult contactless palmprint databases. We show competitive recognition performance of our system as compared against a SOTA COTS system @ FAR=0.1%. The main technical contributions of our paper include a re-alignment strategy for palmprint images using a TPS alignment module and an autoencoder-based image enhancement. Furthermore, we will place our database collection, two child and one adult contactless palmprint databases in public domain once this paper has been accepted. Future work may include i) Child Palm-ID mobile app displaying the faces of the top N retrievals from a gallery for a probe so the operator is able to manually confirm the identity of the child, ii) introduction of a palmprint image quality metric to filter images of poor quality, iii) multimodal biometric recognition for children, iv) synthetic palmprint generation to amplify the amount of data available for training.

References

[1] "Number of Children Under 5 Years Old." https://ourworldindata.org/grapher/under-5-population.

[2] A. K. Jain, S. S. Arora, K. Cao, L. Best-Rowden, and A. Bhatnagar, "Fingerprint Recognition of Young Children," *IEEE Transactions on Information Forensics and Security*, vol. 12, no. 7, pp. 1501–1514, 2016.

[3] S. Saggese, Y. Zhao, T. Kalisky, C. Avery, D. Forster, L. E. Duarte-Vera, L. A. Almada-Salazar, D. Perales-Gonzalez, A. Hubenko, M. Kleeman, *et al.*, "Biometric Recognition of Newborns and Infants by Non-Contact Fingerprinting: Lessons Learned," *Gates Open Research*, vol. 3, 2019.

[4] J. J. Engelsma, D. Deb, K. Cao, A. Bhatnagar, P. S. Sudhish, and A. K. Jain, "Infant-ID: Fingerprints for Global Good," *IEEE Transactions on Pattern Analysis and Machine Intelligence*, vol. 44, no. 7, pp. 3543–3559, 2021.

[5] T. Kalisky, S. Saggese, Y. Zhao, D. Johnson, M. Azarova, L. E. Duarte-Vera, L. A. Almada-Salazar, D. Perales-Gonzalez, E. Chacon-Cruz, J. Wang, *et al.*, "Biometric Recognition of Newborns and Young Children for Vaccinations and Health Care: a Non-randomized prospective clinical trial," *Scientific Reports*, vol. 12, no. 1, p. 22520, 2022.

[6] E. Liu, "Infant Footprint Recognition," in *Proceedings of the IEEE International Conference on Computer Vision*, pp. 1653–1660, 2017.

[7] J. Kotzerke, S. Davis, R. Hayes, and K. Horadam, "Newborn and Infant Discrimination: Revisiting Footprints," *Australian Journal of Forensic Sciences*, vol. 51, no. 1, pp. 95–108, 2019.

[8] D. Yambay, M. Johnson, K. Bahmani, and S. Schuckers, "A Feasibility Study on Utilizing Toe Prints for Biometric Verification of Children," in *2019 International Conference on Biometrics (ICB)*, pp. 1–7, IEEE, 2019.

[9] A. Uhl and P. Wild, "Comparing verification performance of kids and adults for fingerprint, palmprint, hand-geometry and digitprint biometrics," in *2009 IEEE 3rd International Conference on Biometrics: Theory, Applications, and Systems*, pp. 1–6, IEEE, 2009.

[10] R. Ramachandra, K. B. Raja, S. Venkatesh, S. Hegde, S. D. Dandappanavar, and C. Busch, "Verifying the Newborns Without Infection Risks Using Contactless Palmprints," in *2018 International Conference on Biometrics (ICB)*, pp. 209–216, IEEE, 2018.

[11] K. Rajaram, A. Devi, and S. Selvakumar, "PalmNet: A CNN Transfer Learning Approach for Recognition of Young Children Using Contactless Palmprints," in *Machine Learning and Autonomous Systems*, pp. 609–622, Springer, 2022.

[12] UIDAI, "Aadhaar Enrolment - Unique Identification Authority of India: Government of India." .

[13] A. K. Jain, A. A. Ross, and K. Nandakumar, *Introduction to Biometrics*. Springer Publishing Company, 2011.

[14] "Amazon One," *Amazon*. https://one.amazon.com/.

[15] "Biometric Authentication Solutions," *Fujitsu Global*. https://www.fujitsu.com/global/services/security/offerings /biometrics/palmsecure/.

[16] "PalmID - Palmprint Biometrics for Devices with Camera," *RedRock Biometrics*, Apr 2023. https://www.redrockbiometrics.com/.

[17] S. A. Grosz and A. K. Jain, "AFR-Net: Attention-Driven Fingerprint Recognition Network," *arXiv preprint arXiv:2211.13897*, 2022.

[18] R. P. Lemes, O. R. Bellon, L. Silva, and A. K. Jain, "Biometric Recognition of Newborns: Identification Using Palmprints," in *2011 International Joint Conference on Biometrics (IJCB)*, pp. 1–6, IEEE, 2011.

[19] C. F. Dosman, D. Andrews, and K. J. Goulden, "Evidence-based Milestone Ages as a Framework for Developmental Surveillance," *Paediatrics & Child Health*, vol. 17, no. 10, pp. 561–568, 2012.

[20] "Aadhaar 2.0 - Ushering the Next Era of Digital Identity and Smart Governance Workshop from 23rd to 25th November, 2021."

[21] Z. Sun, T. Tan, Y. Wang, and S. Li, "Ordinal Palmprint Representation for Personal Identification," in *Proceedings of the IEEE Conference on Computer Vision and Pattern Recognition*, 2005.

[22] "Products Powered by Armatura." .

[23] L. Dian and S. Dongmei, "Contactless Palmprint Recognition Based on Convolutional Neural Network," in *IEEE 13th International Conference on Signal Processing (ICSP)*, pp. 1363–1367, IEEE, 2016.

[24] L. Zhang, L. Li, A. Yang, Y. Shen, and M. Yang, "Towards Contactless Palmprint Recognition: A Novel Device, a New Benchmark, and a Collaborative Representation Based Identification Approach," *Pattern Recognition*, vol. 69, pp. 199–212, 2017.

[25] Y. Liu and A. Kumar, "Contactless Palmprint Identification Using Deeply Learned Residual Features," *IEEE Transactions on Biometrics, Behavior, and Identity Science*, vol. 2, no. 2, pp. 172–181, 2020.

[26] A. Morales, M. A. Ferrer, and A. Kumar, "Towards Contactless Palmprint Authentication," *IET Computer Vision*, vol. 5, no. 6, pp. 407–416, 2011.

[27] X. Wu, Q. Zhao, and W. Bu, "A SIFT-based Contactless Palmprint Verification Approach Using Iterative RANSAC and Local Palmprint Descriptors," *Pattern Recognition*, vol. 47, no. 10, pp. 3314–3326, 2014.

[28] L. Leng, M. Li, C. Kim, and X. Bi, "Dual-source Discrimination Power Analysis for Multi-instance Contactless Palmprint Recognition," *Multimedia Tools and Applications*, vol. 76, no. 1, pp. 333–354, 2017.

[29] E. Liu, A. K. Jain, and J. Tian, "A Coarse to Fine Minutiae-based Latent Palmprint Matching," *IEEE Transactions on Pattern Analysis and Machine Intelligence*, vol. 35, no. 10, pp. 2307–2322, 2013.

[30] A. K. Jain and J. Feng, "Latent Palmprint Matching," *IEEE Transactions on Pattern Analysis and Machine Intelligence*, vol. 31, no. 6, pp. 1032–1047, 2008.

[31] N. Duta, A. K. Jain, and K. V. Mardia, "Matching of Palmprints," *Pattern Recognition Letters*, vol. 23, no. 4, pp. 477–485, 2002.

[32] Y. Wu and Q. Ji, "Facial Landmark Detection: A Literature Survey," *International Journal of Computer Vision*, vol. 127, pp. 115–142, 2019.

[33] Z. Zhang, P. Luo, C. C. Loy, and X. Tang, "Facial Landmark Detection by Deep Multi-Task Learning," in *13th European Conference on Computer Vision, Zurich, Switzerland, September 6-12*, pp. 94–108, Springer, 2014.

[34] C. A. Stevens, J. C. Carey, M. Shah, and G. P. Bagley, "Development of Human Palmar and Digital Flexion Creases," *The Journal of Pediatrics*, vol. 113, no. 1, pp. 128–132, 1988.

[35] S. Kimura and T. Kitagawa, "Embryological Development of Human Palmar, Plantar, and Digital Flexion Creases," *The Anatomical Record*, vol. 216, no. 2, pp. 191–197, 1986.

[36] X. Wu, D. Zhang, K. Wang, and B. Huang, "Palmprint Classification Using Principal Lines," *Pattern Recognition*, vol. 37, no. 10, pp. 1987–1998, 2004.

[37] D. Zhang, W.-K. Kong, J. You, and M. Wong, "Online Palmprint Identification," *IEEE Transactions on Pattern Analysis and Machine Intelligence*, vol. 25, no. 9, pp. 1041–1050, 2003.

[38] H. Zhang and L. Chi, "End-to-End Spatial Transform Face Detection and Recognition," *Virtual Reality & Intelligent Hardware*, vol. 2, no. 2, pp. 119–131, 2020.

[39] J. J. Engelsma, K. Cao, and A. K. Jain, "Learning a Fixed-Length Fingerprint Representation," *IEEE Transactions on Pattern Analysis and Machine Intelligence*, vol. 43, no. 6, pp. 1981–1997, 2019.

[40] C. Bhagavatula, C. Zhu, K. Luu, and M. Savvides, "Faster than Real-time Facial Alignment: A 3D Spatial Transformer Network Approach in Unconstrained Poses," in *Proceedings of the IEEE International Conference on Computer Vision*, pp. 3980–3989, 2017.

[41] S. A. Grosz, J. J. Engelsma, E. Liu, and A. K. Jain, "C2CL: Contact to Contactless Fingerprint Matching," *IEEE Transactions on Information Forensics and Security*, vol. 17, pp. 196–210, 2021.

[42] W. Li, D. Zhang, and Z. Xu, "Palmprint Identification by Fourier Transform," *International Journal of Pattern Recognition and Artificial Intelligence*, vol. 16, no. 04, pp. 417–432, 2002.

[43] A. Jalali, R. Mallipeddi, and M. Lee, "Deformation Invariant and Contactless Palmprint Recognition using Convolutional Neural Network," in *Proceedings of the 3rd International Conference on Human-agent Interaction*, pp. 209–212, 2015.

[44] Y. Liu and A. Kumar, "A Deep Learning Based Framework to Detect and Recognize Humans Using Contactless Palmprints in the Wild," *arXiv preprint arXiv:1812.11319*, 2018.

[45] X. Liang, J. Yang, G. Lu, and D. Zhang, "CompNet: Competitive Neural Network for Palmprint Recognition Using Learnable Gabor Kernels," *IEEE Signal Processing Letters*, vol. 28, pp. 1739–1743, 2021.

[46] Y. Hao, Z. Sun, T. Tan, and C. Ren, "Multispectral Palm Image Fusion for Accurate Contact-Free Palmprint Recognition," in *2008 15th IEEE International Conference on Image Processing*, pp. 281–284, IEEE, 2008.

[47] "COEP Palm Print Database," *COEP Palm Print Database — College of Engineering, Pune*. https://www.coep.org.in/resources/coeppalmprintdatabase.

[48] M. Izadpanahkakhk, S. M. Razavi, M. Taghipour-Gorjikolaie, S. H. Zahiri, and A. Uncini, "Novel Mobile Palmprint Databases for Biometric Authentication," *International Journal of Grid and Utility Computing*, vol. 10, no. 5, pp. 465–474, 2019.

[49] S. A. Grosz and A. K. Jain, "Latent Fingerprint Recognition: Fusion of Local and Global Embeddings," *arXiv preprint arXiv:2304.13800*, 2023.

[50] K. He, X. Zhang, S. Ren, and J. Sun, "Deep Residual Learning for Image Recognition," in *Proceedings of the IEEE Conference on Computer Vision and Pattern Recognition*, pp. 770–778, 2016.

[51] A. Dosovitskiy, L. Beyer, A. Kolesnikov, D. Weissenborn, X. Zhai, T. Unterthiner, M. Dehghani, M. Minderer, G. Heigold, S. Gelly, J. Uszkoreit, and N. Houlsbyand, "An Image is Worth 16x16 Words: Transformers for Image Recognition at Scale," *arXiv preprint arXiv:2010.11929*, 2020.

[52] O. Sagi and L. Rokach, "Ensemble Learning: A Survey," *Wiley Interdisciplinary Reviews: Data Mining and Knowledge Discovery*, vol. 8, no. 4, p. e1249, 2018.

[53] A. Godbole, K. Nandakumar, and A. K. Jain, "Learning an Ensemble of Deep Fingerprint Representations," *arXiv preprint arXiv:2209.02425*, 2022.

7 Appendix

7.1 Score distributions of Child Palm-ID and the COTS system

As mentioned in section 5.1 of the paper, the sum score fusion of the similarity scores from Child Palm-ID and the COTS matcher provided an additional improvement in accuracy across all evaluation databases. This score fusion was particularly important to show the potential for improvement in the case of Child CrossDB. We show that the performance on Child CrossDB improves from TAR=78.1% (for Child Palm-ID) and TAR=78.22% (for COTS) to TAR=82.02% (Child Palm-ID + COTS), all at FAR=0.1%. The contingency table of genuine and imposter comparisons for both matchers helped understand the potential benefit of fusing their results. Table 1 shows the contingency table for the genuine distribution of Child CrossDB. This shows the number of comparisons where i) both matchers gave the same decision (diagonal entries) and ii) both matchers gave different decisions (cross-diagonal entries). Each decision is binary in terms of match/non-match.

Table 5: Contingency table of Child Palm-ID and COTS on Child CrossDB, pre-fusion.

		COTS	
		Match	Non-Match
CPID[†]	Match	162,696	10,805
CPID[†]	Non-Match	21,810	31,316

[†] *We abbreviate Child Palm-ID as CPID in this table.*

We see that the cross-diagonal elements, where the decisions of the matchers are different, are key to improving the performance after fusion. Ideally, both these numbers would be 0.

The architecture of the COTS system is unknown to us. However, we believe the Child Palm-ID system to be distinct from the COTS while showing competitive accuracy across all evaluations, motivating the fusion of the two. Fig. 1 in this document shows the genuine and impostor distributions of Child Palm-ID and the COTS before the fusion.

Figure 15: Example images of the subjects in Child CrossDB that are responsible for a majority of the errors

It appears that the COTS has higher score separation compared to Child Palm-ID. To fuse the scores, we multiply the Child Palm-ID scores by 100 to have the same score range as the COTS ([0, 100]) and then we simply sum the two scores to obtain the fused result. Fig. 2 shows the score distribution after the fusion ([0, 200]).

We can see that visually, the separation between the genuine and imposter scores has improved compared to the individual distributions of either matcher in Fig. 1. Quantitatively, this results in a higher accuracy for Child CrossDB. We repeat the same fusion technique for all evaluation databases and observe an improvement for each of them at FAR=0.1% (see Table 3. in the paper).

7.2 Additional Failure Cases in Child CrossDB

The primary reason for the lower performance of both Child Palm-ID and the COTS is due to the underlying differences in the nature of the two child palmprint databases, Child-PalmDB1 and Child-PalmDB2. The images in Child-PalmDB1 contain a much larger variation in pose, higher standoff distances and lower image quality compared to Child-PalmDB2. We look at some of the subjects in Child CrossDB that cause most of the errors in classification in Fig. 15. The top row is images from Child-PalmDB2 and the bottom row is images from Child-PalmDB1. We can see that the causes of error range from large stand-off distances to the hand being covered in henna, etc.
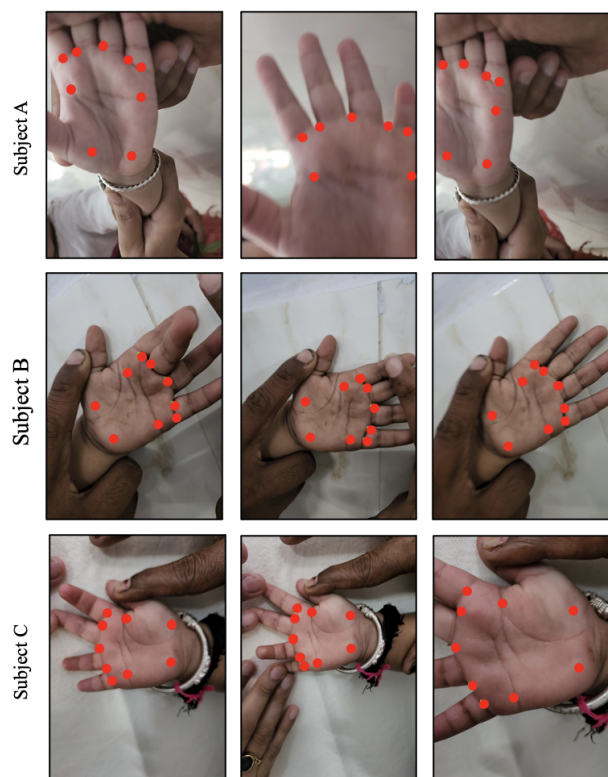
Figure 16: Sample images from three distinct identities having large intra-class variability in terms of occlusion, blurring and stand-off distance.

7.3 Subjects With Large Intra-Class Variability

Due to the continuous capture of images in PalmMobile SDK Android application coupled with the uncooperative nature of the subjects results in a large intra-class variability. This includes blurring, half-open fists and occlusions from the operator's hand and other background elements due to the unexpected movement of the subjects. Fig. 16 shows examples of 3 distinct palms having images with larger intra-class variability. It is in these cases where the number of misclassified samples increases.